Angular distributions from two-photon detachment of H^- near ionization threshold: Laser-frequency and -intensity effects

Dmitry A. Telnov* and Shih-I Chu
Department of Chemistry, University of Kansas, Lawrence, Kansas 66045
and Kansas Center for Advanced Scientific Computing, Lawrence, Kansas 66045
(Received 10 June 2002; published 18 December 2002)

We have performed a nonperturbative Floquet study of the angular distributions of the emitted electrons in the two-photon detachment of H^- driven by strong infrared laser fields. The external field parameters are chosen to correspond to the recent experiment by R. Reichle, H. Helm, and I. Yu. Kiyan, Phys. Rev. Lett. **87**, 243001 (2001). We discuss the laser-frequency and -intensity effects on the shape of the angular distribution in the vicinity of the ionization threshold. We show that the angular distribution pattern can be interpreted in terms of the interference of the *s* and *d* partial waves in the final state and the Wigner threshold law.

DOI: 10.1103/PhysRevA.66.063409 PACS number(s): 32.80.Rm, 32.80.Gc

In a recent experimental work, Reichle, Helm, and Kiyan [1] reported on the intensity-resolved electron angular distributions (AD) from the two-photon detachment of H^- by the 2.15-μm infrared laser field. They discovered dramatic changes in AD with increasing intensity of the laser field. Particularly, at the intensity 6.5×10^{11} W/cm^2, AD has a bell shape with the maximum pointing perpendicular to the laser polarization. To explain this behavior, the authors of Ref. [1] make use of an extension [2] of the earlier semiclassical Keldysh-Faisal-Reiss (KFR) theory [3]. In the present paper we extend the non-Hermitian Floquet theory [4] for quantum investigation of the mechanism responsible for the observed AD phenomenon. We found that AD can be well described in terms of the interference of the lowest partial waves, as predicted by the perturbation theory and the Wigner threshold law [5]. Moreover, the phenomenon is not directly due to the effect of the strong laser field, and can be observed in principle at much lower intensities than those used in the experiment [1] as well.

The study of multiphoton and above-threshold detachment processes of the H^- ion has attracted much interest both experimentally and theoretically in the last decade. The short-range interaction between the outer electron and the core supports only one bound state. Further, under the experimental conditions [1,6,7] for which the laser frequencies are either smaller or comparable to the binding energy of the H^- ion, doubly excited states lie far above the detachment threshold and can be safely ignored. This simplifying feature renders the multiphoton and above-threshold detachment of H^- a unique and fundamental process to study.

We describe the H^- ion by an accurate one-electron model constructed [8] to reproduce both the exact experimental binding energy [9] and the low-energy e-H(1s) elastic scattering phase shifts [10,11]. The one-photon detachment cross sections based on this model potential are in excellent agreement with earlier accurate two-electron calculations [11,12]. Detailed Floquet studies of the frequency- and intensity-dependent multiphoton detachment of H^- [13] using this model potential were in good agreement with the Los Alamos experimental data [14], as well as the two-electron *R*-matrix Floquet calculation [15]. Our recent nonperturbative Floquet study of the electron AD associated with the above-threshold multiphoton detachment of H^- by 1064-nm laser field [16] and that of the two-photon AD near the one-photon threshold [17], again using this model potential, is also in good harmony with the recent experimental work in Los Alamos [7] and Aarhus [6], respectively. The angle-integrated multiphoton detachment rates, presented in the same work [16,17], agree well with the recently performed two-electron calculations [18].

In the present nonperturbative Floquet studies we make use of the complex scaling–generalized pseudospectral (CS-GPS) method for the *nonuniform* spatial discretization and solution of the non-Hermitian Floquet Hamiltonian. The CS-GPS method is found to be both accurate and computationally efficient, and is applicable to both low-lying and highly excited atomic and molecular resonance states. The details of the method can be found elsewhere for the *uniform* complex scaling [13,19] and *exterior* complex scaling procedures [17].

The procedure for the calculation of electron energy and angular distributions within the Floquet formalism has been described elsewhere [16,17]. Here we outline the basic formulas for the description of multiphoton detachment of H^-. In the presence of linearly polarized monochromatic fields, the expression for the electron AD after absorption of n photons can be written [16] as

$$\frac{d\Gamma_n}{d\Omega}=(2\pi)^{-2}k_n|A_n(\boldsymbol{k}_n)|^2. \qquad (1)$$

Here $A_n(\boldsymbol{k}_n)$ is the n-photon detachment amplitude [16], and

$$k_n=\sqrt{2[\mathrm{Re}\,\varepsilon-(2\omega)^{-2}F^2+n\omega]} \qquad (2)$$

is the electron drift momentum, ε, $\boldsymbol{F}$, and ω being the (complex) quasienergy, laser field strength and frequency, respectively. The quantity $d\Gamma_n/d\Omega$ represents the number of elec-

*Permanent address: Department of Physics, St. Petersburg State University, 198904 St. Petersburg, Russia. Electronic address: telnov@pcqnt1.phys.spbu.ru

trons per unit time detached with absorption of n photons and emitted within the unit solid angle under direction of the vector $\boldsymbol{k}_n$. Integration of AD (1) with respect to the angles specifying the direction $\boldsymbol{k}_n$ gives the partial rates Γ_n:

$$\Gamma_n = \int d\Omega \frac{d\Gamma_n}{d\Omega}. \tag{3}$$

One can expand $d\Gamma_n/d\Omega$ as a function of the angle θ between the detection $\boldsymbol{k}_n$ and field $\boldsymbol{F}$ directions on the basis of the Legendre polynomials. Due to parity restrictions, only even Legendre polynomials are present in the expansion:

$$\frac{d\Gamma_n}{d\Omega} = \frac{\Gamma_n}{4\pi}\left(1 + \sum_{l=1}^{\infty} \beta_{2l}^{(n)} P_{2l}(\cos\theta)\right). \tag{4}$$

Here $\beta_{2l}^{(n)}$ are the anisotropy parameters. If all $\beta_{2l}^{(n)}$ are zero, AD (4) is isotropic. When analyzing the behavior of AD for weak and medium-strong external fields, a comparison with the results of the lowest-order perturbation theory (LOPT) is valuable. For the two-photon detachment, according to LOPT, the emitted electrons may possess the angular momentum of 0 or 2, that is s and d waves are mixed in the final state. Then the dependence of the detachment amplitude A_2 on the angle θ can be expressed as follows:

$$\delta\sqrt{\frac{1}{2}}P_0(\cos\theta) + \sqrt{\frac{5}{2}}P_2(\cos\theta), \tag{5}$$

the factors $\sqrt{1/2}$ and $\sqrt{5/2}$ being added as normalization coefficients for the Legendre polynomials. The mixing coefficient δ is a complex number; in general, it depends not only on the angular algebra, but also on the radial wave functions. Using Eq. (5) in the calculation of AD [Eqs. (1) and (4)], one can find a relation between the parameters $\beta_{2l}^{(2)}$ and the mixing coefficient δ:

$$\beta_2^{(2)} = \frac{10 + 14\,\mathrm{Re}\,\delta\sqrt{5}}{7(1+|\delta|^2)}, \quad \beta_4^{(2)} = \frac{18}{7(1+|\delta|^2)}, \tag{6}$$

other parameters $\beta_{2l}^{(2)}$ being zero within LOPT. Note that the analysis of AD based on the mixing coefficient δ is applicable if the only significant contributions to the two-photon detachment amplitude are from s and d waves, i.e., in the case of weak and medium-strong external fields. For very strong external fields, the general approach based on the anisotropy parameters $\beta_{2l}^{(2)}$ should be used.

Using our nonperturbative Floquet-CSGPS approach with exterior complex scaling [17], we have calculated AD of the emitted electrons after the two-photon detachment of H^-. Two sets of the calculations have been performed. First, we computed AD for the low laser field intensity 1×10^9 W/cm^2 and the number of frequencies between the one- and two-photon detachment thresholds (0.0277 a.u. and 0.0139 a.u., respectively, in the weak-field limit). Second, for the selected laser wavelength of 2.15 μm (frequency 0.0212 a.u.) used in the experiment [1], AD were computed for several laser field intensities in the range (1×10^9)–(6.5×10^{11}) W/cm^2. For the first set of the calculations, the results are presented in Fig. 1 and Table I.

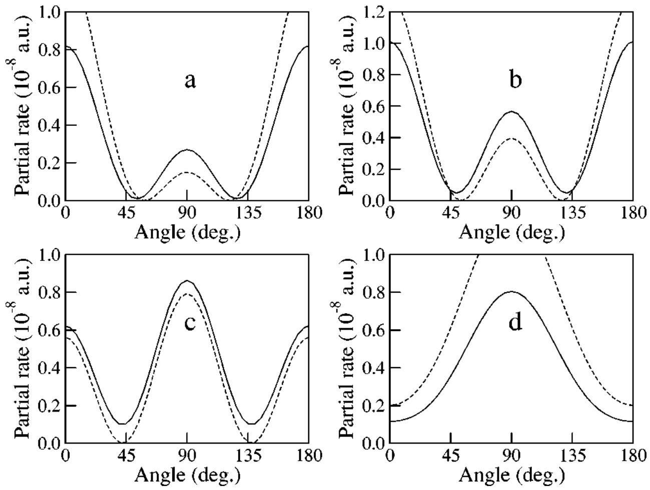

FIG. 1. Angular distributions for two-photon detachment of H^-. The laser field intensity is 1×10^9 W/cm^2. The laser field frequency is (a) 0.026 a.u., (b) 0.021 a.u. (2.15 μm wavelength), (c) 0.018 a.u., and (d) 0.015 a.u. The solid line represents present results; the dashed line represents theory [2].

As one can see from Fig. 1, the shape of AD changes dramatically with the external field frequency when the two-photon threshold is approached. Very close to the threshold, at the frequency 0.015 a.u. AD has the bell shape with the maximum at $\theta = 90°$, quite similar to that observed in the experiment [1]. Since no strong-field effect is involved at such a low intensity, the explanation of the phenomenon can be provided within LOPT, that means only the interference of s and d partial waves is responsible for the changing AD. It is the Wigner threshold law [5] that plays a key role here. According to this law, the d wave contribution to the two-photon detachment amplitude A_2 scales as k_2^4 when $k_2 \to 0$, while the s-wave contribution remains finite in this limit and hence dominates the detachment amplitude and partial rate in the vicinity of the threshold. The computed values of the mixing coefficient δ (see Table I) confirm this observation. The relative output P_s of s electrons calculated as $P_s = |\delta|^2/(1+|\delta|^2)$ changes from 0.056 at the frequency 0.026 a.u. to 0.928 at the frequency 0.015 a.u. Note that interference of s and d partial waves near the two-photon threshold is responsible also for the structure in the frequency and intensity dependence of the *angle-integrated* two-photon detachment rates, as was discussed in the literature [18,20].

Now turn to the second set of our calculations, which were performed for the laser wavelength of 2.15 μm and the

TABLE I. Mixing coefficient δ for the two-photon detachment of H^- at the intensity 1×10^9 W/cm^2.

	Laser field frequency (a.u.)			
	0.015	0.018	0.021	0.026
$\lvert\delta\rvert$	3.59	0.973	0.522	0.244
Re δ	−3.31	−0.718	−0.303	−0.096

TABLE II. Anisotropy parameters $\beta_{2l}^{(2)}$ and the mixing coefficient δ for the two-photon detachment of H^- by the laser field with the wavelength 2.15 μm. (A) represents present calculations; (B) represents Ref. [2]. The numbers in brackets indicate powers of 10.

	Laser field intensity (W/cm^2)				
	1.0[9]	1.0[10]	1.3[11]	4.0[11]	6.5[11]
(A) $\beta_2^{(2)}$	5.70[−2]	3.06[−2]	−3.62[−1]	−1.30	−1.19
(B) $\beta_2^{(2)}$	1.04	9.89[−1]	2.35[−1]	−1.43	−1.37
(A) $\beta_4^{(2)}$	2.02	2.01	1.84	1.16	2.87[−1]
(B) $\beta_4^{(2)}$	2.58	2.57	2.41	1.47	3.92[−1]
(A) $\beta_6^{(2)}$	−4.14[−4]	−4.14[−3]	−4.18[−2]	−4.88[−2]	−7.71[−3]
(B) $\beta_6^{(2)}$	5.99[−2]	5.54[−2]	3.40[−3]	−3.94[−2]	−1.08[−2]
(A) $\beta_8^{(2)}$	−4.24[−8]	3.64[−6]	3.95[−4]	−8.69[−4]	9.10[−5]
(B) $\beta_8^{(2)}$	8.87[−3]	8.59[−3]	5.89[−3]	2.33[−3]	2.67[−4]
(A) $\lvert\delta\rvert$	5.22[−1]	5.29[−1]	6.33[−1]	1.10	2.82
(A) Re δ	−3.03[−1]	−3.11[−1]	−4.33[−1]	−9.65[−1]	−2.70

intensities 1×10^{10}, 1.3×10^{11}, 4×10^{11}, and 6.5×10^{11} W/cm^2. Table II contains the anisotropy parameters $\beta_{2l}^{(2)}$ and the mixing coefficient δ. As one can see, even for the intensities as high as 4×10^{11} and 6.5×10^{11} W/cm^2, AD can be well described by a superposition of s and d partial waves in the two-photon detachment amplitude. The parameters $\beta_6^{(2)}$ and $\beta_8^{(2)}$ that account for the higher angular momenta, are quite small compared with $\beta_2^{(2)}$ and $\beta_4^{(2)}$. Again, it is the Wigner threshold law that determines the behavior of the detachment amplitude in the vicinity of the two-photon threshold. In the first set of our calculations (Table I), the electron drift momentum k_2 after absorption of two photons is tuned in the vicinity of the threshold by changing the laser frequency [see Eq. (2)] since the ac Stark shift of the quasienergy and the ponderomotive shift of the onset of the continuum (or the electron quiver energy in the field) $U_p=(2\omega)^{-2}F^2$ are negligible at the intensity 1×10^9 W/cm^2. In the second set (Table II), the latter quantities become important with increasing intensity. When the laser intensity increases with the frequency fixed, the larger ac Stark and ponderomotive shifts bring the electron drift momentum k_2 in the vicinity of the two-photon detachment threshold. This changes the relative contribution of the s and d waves in the detachment amplitude (see Table II for the mixing coefficient δ), and as a consequence, the shape of AD. This is the only intensity effect on AD for the laser intensity range under consideration. Generally, AD pattern for the second set (Fig. 2) resembles that for the first set (Fig. 1).

In Figs. 1 and 2 and Table II we also show the results of the KFR-like theory of Ref. [2], which was used in Ref. [1] to explain the experimental data. The theory [2] is an approximate adiabatic theory valid for large number of photons absorbed in the detachment process. Caution should be exercised when applying this theory to the two-photon detachment since the results may contain a significant error. Figure 1 contains (not scaled) AD from the theory [2]. As one can see, while the shapes of those AD are close to the present results, the magnitudes may differ significantly for particular angles. The angle-integrated two-photon detachment rates from the theory [2], as our calculations show, differ as much as 20% from the present results. (the 60% difference for the frequency 0.015 a.u. can be explained by the fact that in the close vicinity of the threshold, the rate is very sensitive to the position of the quasienergy level, and the theory [2] does not take the quasienergy shift into account). Strictly speaking, AD of the theory [2] are inaccurate in the LOPT limit since they still contain contributions of the higher angular momenta, which are supposed to vanish as predicted by LOPT. The results presented in Table II confirm these observations. As one can see, the anisotropy parameters, calculated using the present theory based on the accurate model potential for H^- and nonperturbative Floquet approach, differ much from those from the theory [2] for weak and medium-strong laser fields. Only for the highest intensities (4×10^{11} and 6.5×10^{11} W/cm^2) used in the calculations, in the vicinity of the two-photon threshold, the present results and that of Ref. [2] get closer to each other.

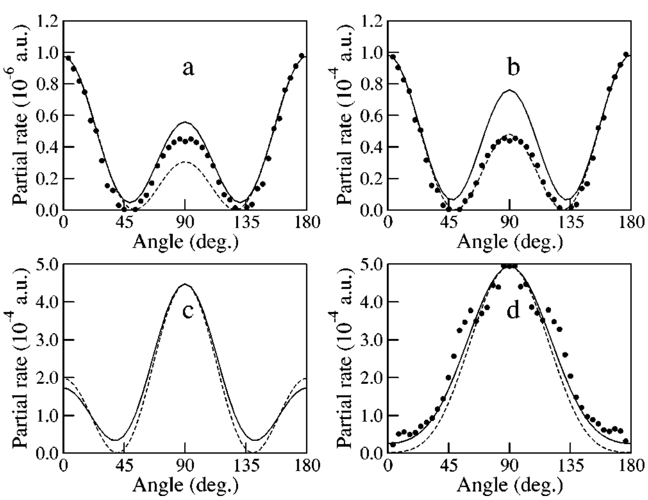

FIG. 2. Angular distributions for two-photon detachment of H^-. The wavelength of the laser field is 2.15 μm. The laser field intensity is (a) 1×10^{10} W/cm^2, (b) 1.3×10^{11} W/cm^2, (c) 4×10^{11} W/cm^2, and (d) 6.5×10^{11} W/cm^2. The solid line represents the present results; and the dashed line the theory [2] scaled to match the maxima of the present AD. The black dots represent the experimental data [1] attributed to the intensity 6.5×10^{11} W/cm^2 in (d) and 1.3×10^{11} W/cm^2 in (a) and (b).

In Fig. 2, for the purpose of comparison of AD shapes, the results of the theory [2] and experimental data [1] are scaled to match the maxima of our computed AD. AD presented in Ref. [1] were attributed to the intensities 1.3×10^{11} and 6.5×10^{11} W/cm^2. We reproduce them in Figs. 2(b) and 2(d), respectively. As one can see, at the intensity 6.5×10^{11} W/cm^2 the experimental AD are in good agreement with the present calculations as well as with the theory [2]. Agreement between the experimental and our theoretical results is not that good at the intensity 1.3×10^{11} W/cm^2 [Fig. 2(b)], particularly near the central maximum of AD at 90°. The agreement with the experimental data is better for the theory [2]. However, our theory is more accurate than the semiclassical theory [2] used beyond its validity region. To explain this discrepancy, one can notice that rapid changes in AD shape begin when the intensity reaches approximately 1×10^{11} W/cm^2 [compare Figs. 2(b)–2(d)]. That is why even small inaccuracy in determination of the intensity in this region can lead to a large difference in the AD shape. Note that the same experimental data attributed by the authors of Ref. [1] to the intensity 1.3×10^{11} W/cm^2 match much better our theoretical curve for the lower intensity 1×10^{10} W/cm^2 [see Fig. 2(a)]. So, we can suggest that the intensity measurement at 1.3×10^{11} W/cm^2 in Ref. [1] may be not that accurate (for example, the ac Stark shift was not taken into account when the intensity was determined through the ponderomotive shift, and it constitutes about 10% of the ponderomotive shift for the laser frequency and intensities under consideration), and AD presented for this intensity [1] in reality correspond to a weaker laser field. In this regard, further experimental investigation would be desirable.

In conclusion, we have presented nonperturbative Floquet study of electron AD after two-photon detachment of H^- negative ion. Our analysis shows that for the laser field intensities up to 6.5×10^{11} W/cm^2, AD exhibit only interference of *s* and *d* partial waves in the final state of the photoelectron. The shape of AD for the fixed laser wavelength 2.15 μm does not change significantly as the intensity increases from zero to approximately 1×10^{11} W/cm^2. For larger laser field intensities, the ponderomotive and ac Stark shifts bring the two-photon detachment channel closer to the threshold, and the shape of AD changes in accordance with the Wigner threshold law, manifesting the increase of the relative weight of the *s* electrons. The same effect can be observed when the laser field intensity is fixed and the frequency varies. We demonstrate it for as low intensity as 1×10^9 W/cm^2 where the perturbation theory applies.

This work was partially supported by NSF Grant No. 0098106. We acknowledge the Kansas Center for Advanced Scientific Computing for the support of Origin2400 supercomputer time.

[1] R. Reichle, H. Helm, and I.Yu. Kiyan, Phys. Rev. Lett. **87**, 243001 (2001).
[2] G.F. Gribakin and M.Yu. Kuchiev, Phys. Rev. A **55**, 3760 (1997).
[3] L.V. Keldysh, Zh. Éksp. Teor. Fiz. **47**, 1945 (1964) [Sov. Phys. JETP **20**, 1307 (1965)]; F.H.M. Faisal, J. Phys. B **6**, L89 (1973); H.R. Reiss, Phys. Rev. A **22**, 1786 (1980).
[4] S.I. Chu, Adv. Chem. Phys. **73**, 739 (1989).
[5] E.P. Wigner, Phys. Rev. **73**, 1002 (1948).
[6] L. Præstegaard, T. Andersen, and P. Balling, Phys. Rev. A **59**, R3154 (1999).
[7] X.M. Zhao, M.S. Gulley, H.C. Bryant, C.E.M. Strauss, D.J. Funk, A. Stintz, D.C. Rislove, G.A. Kyrala, W.B. Ingalls, and W.A. Miller, Phys. Rev. Lett. **78**, 1656 (1997).
[8] C. Laughlin and S.I. Chu, Phys. Rev. A **48**, 4654 (1993).
[9] K.R. Lykke, K.K. Murray, and W.C. Lineberger, Phys. Rev. A **43**, 6104 (1991).
[10] C. Schwartz, Phys. Rev. **124**, 1468 (1961); M.R.H. Rudge, J. Phys. B **8**, 940 (1975); J. Callaway, Phys. Lett. A **65**, 199 (1978).
[11] A.L. Stewart, J. Phys. B **11**, 3851 (1978).
[12] A.W. Wishart, J. Phys. B **12**, 3511 (1979).
[13] J. Wang, S.I. Chu, and C. Laughlin, Phys. Rev. A **50**, 3208 (1994).
[14] C.Y. Tang, P.G. Harris, H.C. Bryant, A.H. Mohagheghi, R.A. Reeder, H. Sharifian, H. Toutounchi, C.R. Quick, J.B. Donahue, S. Cohen, and W.W. Smith, Phys. Rev. Lett. **66**, 3124 (1991).
[15] M. Dörr, J. Purvis, M. Terao-Dunseath, P.G. Burke, C.J. Joachain, and C.J. Noble, J. Phys. B **28**, 4481 (1995).
[16] D.A. Telnov and S.I. Chu, J. Phys. B **29**, 4401 (1996).
[17] D.A. Telnov and S.I. Chu, Phys. Rev. A **59**, 2864 (1999).
[18] C. Haritos, T. Mercouris, and C.A. Nicolaides, Phys. Rev. A **63**, 013410 (2001).
[19] G. Yao and S.I. Chu, Chem. Phys. **204**, 381 (1993).
[20] C.A. Nicolaides and T. Mercouris, Chem. Phys. Lett. **159**, 45 (1989).